Aesth Plast Surg
https://doi.org/10.1007/s00266-025-05444-0

ORIGINAL ARTICLE BASIC SCIENCE/EXPERIMENTAL

Regenerative Effect of Vaginal Injections of Umbilical Cord Mesenchymal Stem Cell-Derived Exosomes in Ovariectomized Rats



Ya-Wei Lai[1,2,6] · Sheng-Hua Wu[3,4,5] · Ping-Ruey Chou[7,8] · Yu-Chi Wang[1] · Jwu-Lai Yeh[9] · Tsai-Ming Lin[10] · Chee-Yin Chai[11] · Cheng-Hsien Tsai[12] · Shu-Hung Huang[1,13,14]

Received: 15 May 2025 / Accepted: 6 November 2025
© Springer Science+Business Media, LLC, part of Springer Nature and International Society of Aesthetic Plastic Surgery 2025

Abstract

Background In genitourinary syndrome of menopause (GSM), reduced estrogen levels cause several pathological changes in the vaginal mucosa, including epithelial thinning, decreased blood flow and glycogen production, loss of elasticity, and mucus production. Umbilical cord mesenchymal stem cell–derived exosomes (ucMSC-ex) facilitate intercellular communication and play a key role in mucosal regeneration and immune response modulation.

Objectives We examined the therapeutic effect of ucMSC-ex injection on vaginal atrophy in ovariectomized rats.

Methods Tangential flow filtration was used to extract ucMSC-ex. Female Sprague-Dawley rats were divided into three groups: a group receiving sham treatment, a group receiving sham treatment after ovariectomy, and a group receiving vaginal ucMSC-ex injection after ovariectomy. Treatment efficacy was determined by analyzing rat vaginal tissue to observe changes in the vaginal epithelium and

✉ Shu-Hung Huang
huangsh63@gmail.com;
https://www.instagram.com/huangsh63?igsh=MThybzBkcGVvbjZpdw%3D%3D&utm_source=qr

1 Division of Plastic Surgery, Department of Surgery, Kaohsiung Medical University Hospital, Kaohsiung 807, Taiwan

2 Division of Plastic Surgery, Department of Surgery, Kaohsiung Medical University Gangshan Hospital, Kaohsiung 820, Taiwan

3 Department of Anesthesiology, Kaohsiung Medical University Gangshan Hospital, Kaohsiung 820, Taiwan

4 Department of Anesthesiology, Kaohsiung Medical University Hospital, Kaohsiung 807, Taiwan

5 Department of Anesthesiology, School of Medicine, College of Medicine, Kaohsiung Medical University, Kaohsiung 807, Taiwan

6 Graduate Institute of Clinical Medicine, College of Medicine, Kaohsiung Medical University, Kaohsiung 807, Taiwan

7 Graduate Institute of Medicine, College of Medicine, Kaohsiung Medical University, Kaohsiung 807, Taiwan

8 Department of Surgery, Kaohsiung Medical University Hospital, Kaohsiung 807, Taiwan

9 Department of Pharmacology, School of Medicine, College of Medicine, Kaohsiung Medical University, Kaohsiung 807, Taiwan

10 Charming Institute of Aesthetic and Regenerative Surgery (CIARS), 2F.-1, No. 172, Ziqiang 2nd Road, Qianjin District, Kaohsiung 801, Taiwan

11 Departments of Pathology, College of Medicine, Kaohsiung Medical University, Kaohsiung 807, Taiwan

12 BIONET Therapeutics Corp., 1F, No.28, Ln. 36, Xinhu 1st Rd., Neihu Dist., Taipei City 114, Taiwan

13 Professor of Department of Surgery, School of Medicine, College of Medicine, Kaohsiung Medical University, No.100, Tzyou 1st Rd., Sanmin Dist., Kaohsiung 807, Taiwan

14 Division of Plastic Surgery, Department of Surgery, Kaohsiung Municipal Siaogang Hospital, Kaohsiung 812, Taiwan

Published online: 23 November 2025

in collagenesis, angiogenesis, estrogen receptor count, vaginal lubrication, and inflammatory response.
Results Our preliminary histological results indicated that ucMSC-ex injection enhanced structural restoration, collagen formation, angiogenesis, estrogen receptor expression, vaginal lubrication, cellular proliferation, and anti-inflammatory response in vaginal tissue, indicating its regenerative potential as a treatment for GSM.
Conclusions Our findings support the therapeutic potential of exosome therapy in alleviating the symptoms of GSM by promoting tissue regeneration and vascularization, restoring vaginal lubrication, and reducing inflammation.
No Level Assigned This journal requires that authors assign a level of evidence to each submission to which Evidence-Based Medicine rankings are applicable. This excludes Review Articles, Book Reviews, and manuscripts that concern Basic Science, Animal Studies, Cadaver Studies, and Experimental Studies. For a full description of these Evidence-Based Medicine ratings, please refer to the Table of Contents or the online Instructions to Authors www.springer.com/00266.

Keywords Genitourinary syndrome of menopause (GSM) · Umbilical cord mesenchymal stem cell–derived exosomes (ucMSC-ex) · Vaginal rejuvenation · Vaginal lubrication

Introduction

Hypoprogesterone causes various genitourinary problems, commonly in women with genitourinary syndrome of menopause (GSM) and in postpartum women with sexual dysfunction [1]. These problems include external genital atrophy, vaginal atrophy, and stress urinary incontinence [2, 3]. Hypoprogesterone affects approximately 15% of menopausal women and up to 40–54% of postmenopausal women, in addition to certain postpartum women, influencing their vaginal appearance and quality of life [4]. Although treatment involves traditional lubricants to relieve dryness and discomfort, these lubricants cannot change the histology of vaginal atrophy. Systemic or topical hormone therapy can increase mucosal thickness, but long-term use poses a potential risk in patients with breast cancer, endometrial cancer, and cardiovascular diseases [5, 6].

Umbilical cord mesenchymal stem cell-derived exosomes (ucMSC-ex) are extracellular vesicles that carry bioactive molecules, such as proteins, lipids, and nucleic acids, to facilitate intercellular communication [7]. Previous studies have demonstrated the regenerative, tissue healing, and anti-inflammatory properties of exosomes [8]. The regenerative potential of exosomes can be attributed to their growth factors, cytokines, and other signaling molecules that cause angiogenesis [9, 10]. Exosomes have also been observed to promote intestinal mucosal repair, given their role as a key component of the paracellular structure [11].

Exosome-based therapy for vaginal atrophy and dryness remains in its early stages, and few studies have examined the restorative effect of this therapy. In addition, no studies have yet explored the local administration methods of exosome-based therapy to ensure targeted and effective delivery. In this study, we examined the regenerative effect of locally injected ucMSC-ex on tissue remodeling, neocollagenesis, neoangiogenesis, estrogen sensitivity, vaginal lubrication, and anti-inflammation in the atrophic vaginal epithelia of ovariectomized rat models simulating a postmenopausal state.

Materials and Methods

Animal Grouping

Our animal protocols were approved by the Institutional Animal Care and Use Committee of Kaohsiung Medical University (IACUC 112047). A total of 18 healthy adult female Sprague-Dawley rats, weighing 180–200 g each, were housed in plastic cages with soft bedding, subjected to a 12-hour light–dark cycle, and provided with free access to food and water. These rats were randomly divided into three groups (n = 6 per group): sham treatment with phosphate-buffered saline (PBS) injection (N), sham treatment after ovariectomy (OVX), and vaginal injection with ucMSC-ex after ovariectomy (OVX+EXO). Figure 1 presents a schematic diagram of the study design.

Ovariectomized Rat Model

To perform an ovariectomy, both ovaries were surgically removed under anesthesia with 1.5% isoflurane. This procedure was conducted in accordance with Ismail et al. [12]. Rats were placed in a prone position, and a surgical area measuring 2 cm × 3 cm was shaved over their lower backs. A 1-cm incision was bilaterally made approximately one finger-width from the spine to access both ovaries and oviducts through the abdominal cavity, which were carefully ligated using 5-0 Vicryl and excised. After the removal of both ovaries, the incision was closed using 2-0 silk and 5-0 Nylon sutures to ensure proper healing. Throughout the procedure, the rats were closely monitored for any postoperative complications while a safe anesthetic depth was maintained.

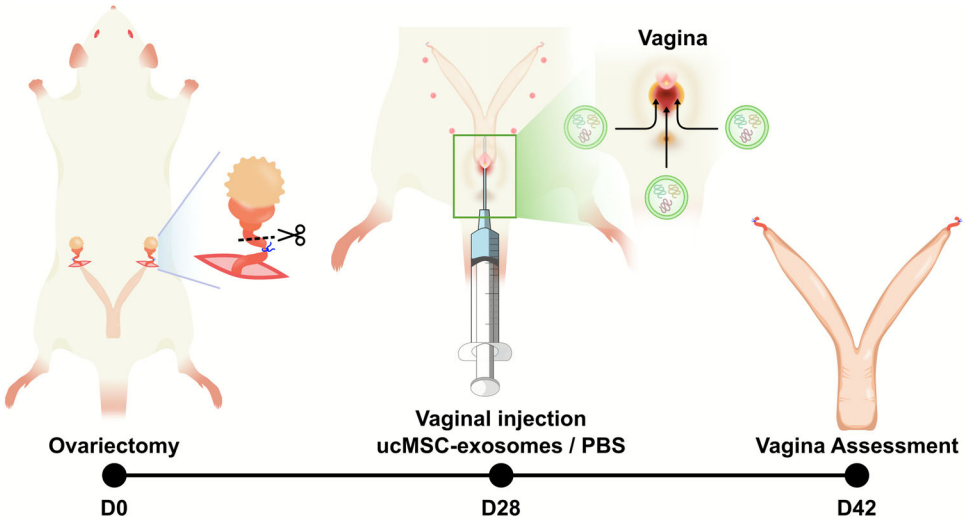


Fig. 1 Experimental timeline and procedure. Ovariectomy was conducted on Day 0 to induce estrogen deficiency in the rat model. On Day 28, a vaginal injection of either ucMSC-ex (treatment) or PBS (control) was administered. On Day 42, histological assessments of vaginal tissue were conducted to evaluate treatment effects

Vaginal Injection of ucMSC-ex

Human ucMSC-ex were acquired from EXOVIA (BIONET Therapeutics, Taipei, Taiwan).

UcMSC-ex Production

Umbilical cord mesenchymal stem cells from a qualified donor were seeded into flasks and cultured in Eagle's minimal essential medium with alpha modification (Gibco, Life Technologies) supplemented with 5% UltraGro (Helios, AventaCell BioMedical) to approximately 80% confluency. Subsequently, the cells were incubated in a serum-free medium at 37 °C for 48 h. Next, the cell culture supernatant was collected, and exosomes were concentrated using tangential flow filtration (Replicon 300K) and sterile-filtered using a 0.22-μm disk filter.

Measurement of ucMSC-ex Size and Concentration Distribution Through Nanoparticle Tracking Analysis

The size distribution and concentration of isolated ucMSC-ex suspensions were analyzed using nanoparticle tracking (PMX-130 ZetaView Mono; Particle Metrix, Germany). All samples were diluted in PBS to a final volume of 1 mL. The optimal particle per frame value (140–200 particles/frame) was pretested to obtain the optimal measurement concentrations. All samples were analyzed in triplicate. After videos were captured, these videos were analyzed using the built-in ZetaView software.

Western Blotting

Cell and exosome samples were lysed with a lysis buffer (Thermo Fisher Scientific) and homogenized with an ultrasonicator (UP-50H; Hielscher GmbH). Protein quantification was performed using a bicinchoninic acid assay kit (Thermo Fisher Scientific). Lysates were diluted with 4× Laemmli Sample Buffer (Bio-Rad Laboratories) and loaded with equal amounts of total protein into sodium dodecyl sulfate polyacrylamide gel electrophoresis gels. Subsequently, the protein was transferred onto a polyvinylidene difluoride membrane with a pore size of 0.45 mm and blocked with 5% nonfat milk for 1 h. Next, the membrane was probed with working concentrations of specific antibodies. Immobilon ECL Ultra Western HRP Substrate (Millipore) and ImageQuant LAS 4000 (GE Healthcare) were used to detect protein bands.

Flow Cytometry

Exosomes were pulled down using magnetic beads coated with CD81 antibodies (10622D; Thermo Fisher Scientific) following manufacturer instructions. Bead–exosome complexes were rinsed and stained with CD9, CD63, or CD81 antibodies for 45 min at room temperature before analysis. The following antibodies and corresponding isotypes were used: CD9-PE (BD Pharmingen, cat# 555372), CD63-PE (BD Pharmingen, cat# 556020), CD81-PE (BD Pharmingen, cat# 555676), and IgG1k-PE (BD Pharmingen, cat# 555749). A BD FACSLyric Flow Cytometer (BD Biosciences) was used to detect exosomes.

Cryo-Electron Microscopy

Quantifoil R1.2/1.3 300-mesh grids with a 2-nm continuous carbon film were glow-discharged using a GloQube Plus system for 80 s at 30 mA. Subsequently, a 4-μL drop of the exosome sample was applied to the grids and blotted for 2 s by using a Vitrobot Mark IV (Thermo Fisher Scientific) with a blot force of −4 at 4 °C and 100% relative humidity. Grids were plunged into liquid nitrogen-cooled

ethane. Movies were collected using EPU (Thermo Fisher Scientific) on a GlaciosCryo-EM (Thermo Fisher Scientific) operated at 200 kV and equipped with a Falcon 4 detector (Thermo Fisher Scientific). Next, exosome movies were collected at a magnification of 92,000× in counting mode with a pixel size of 1.6 Å/pixel. To measure the Feret diameters of the exosomes, cryo-electron microscopy images were analyzed using ImageJ (NIH).

UcMSC-ex Injection

At 4 weeks after surgery, the rats were anesthetized using isoflurane at a concentration of 2–3% in oxygen. Next, ucMSC-ex were directly injected into the submucosal layer of the vaginal wall, a key site for therapeutic activity. A 24-gauge needle was used to select three distinct injection sites at the 3, 6, and 9 o'clock positions around the vaginal circumference for even exosome distribution. Each site received a 0.2-mL injection, ensuring adequate dosing and adherence to the anatomical considerations of the tissue. This submucosal injection procedure enabled proximity to blood vessels and lymphatics, increasing the uptake and bioavailability of exosomes in the target area.

Tissue Specimens

Rat recovery was monitored after injection. At 6 weeks after injection, the rats were euthanized in accordance with ethical guidelines, and vaginal tissues were collected for a subsequent analysis of the therapeutic effects and biological activity of the previously administered ucMSC-ex.

Exosome Marker Assessment

A 500-μL sample was added to a Nanosep, centrifuged at 14,000 ×*g* and 4 °C for 10 min, and recovered through the application of 20-μL PBS on the membrane. Subsequently, ucMSC-ex were labeled with PKH67 (Sigma-Aldrich, St. Louis, MO, USA). Finally, 3 μL of PKH26 dye was mixed with 500 μL of Diluent C, which was combined with the sample, pipetted for 30 s, and allowed to stand at room temperature for 5 min.

Immunohistochemical Staining

At week 6 after injection, tissue specimens were fixed in 10% formalin and embedded in paraffin. A microtome was used to section the paraffin-embedded specimens into slices with a thickness of 5 μm. An immunohistochemical (IHC) analysis was conducted using the streptavidin–biotin method to detect the expression of estrogen receptors (ERs), Ki67, inducible nitric oxide synthase (iNOS), CD34, vascular endothelial growth factor (VEGF), aquaporin 3 (Aqp3), and collagen through Masson's trichrome staining. Subsequently, the specimens were deparaffinized and rehydrated before treatment with 0.1 M citrate buffer (pH 6.0) in an autoclave at 121 °C for 8 min. Next, they were incubated in 3% hydrogen peroxide at room temperature for 5 min to inhibit their endogenous peroxidase activity. After the sections were washed with Tris-buffered saline, they were incubated for 1 h at room temperature with primary antibodies specific to ERs (1:200; Dako, Glostrup, Denmark), Ki67 (1:200, MA5-14520; Invitrogen), iNOS (1:200, GTX130246; GeneTex), CD34 (1:200; Dako), VEGF (1:200, AP629b; Abcepta), Aqp3 (1:200; Arigo), and Masson's trichrome. Subsequently, the specimens were treated with biotinylated secondary antibodies for 30 min and incubated with peroxidase-conjugated streptavidin for an additional 30 min. Primary antibodies were detected using a REAL EnVision Detection System (Dako). Next, the sections were immersed in 3,3′-diaminobenzidine for 5 min, counterstained with hematoxylin to reveal tissue morphology, and mounted on microscope slides. Finally, semiquantitative analyses were independently conducted by two pathologists to determine the expression levels of all markers. Imaging was conducted using an upright microscope (Nikon Ci-L Plus) equipped with a camera (Liweng 800 LITE 4K). Image-Pro Plus 6.0 software was used to quantify expression intensity and merging percentages.

Statistical Analysis

All statistical analyses were conducted using SPSS version 14.0 for Windows (SPSS, Chicago, IL, USA). Each sample was measured in triplicate. Data are expressed as mean [standard error of the mean]. The results of hematoxylin and eosin (H&E) staining, Masson's trichrome, and IHC staining were analyzed using a paired *t* test. A *P* value less than 0.05 was considered statistically significant.

Results

Characterization of ucMSC-ex

Various techniques were used to characterize ucMSC-ex (Fig. 2). Nanoparticle tracking analysis revealed a unimodal size distribution and a median diameter of 112.3 nm for the exomes (Fig. 2A). The peak concentration of the isolated exosomes was determined to be 9.0E+6 particles/mL. Western blotting (Fig. 2B) confirmed the presence of the exosomal markers Alix, TSG101, and CD9 in the ucMSC-ex samples, indicating successful exosome isolation. The intensity of the bands corresponding to Alix, TSG101, and CD9 was considerably higher in the ucMSC-ex lane than in the ucMSC lysate lane, further supporting

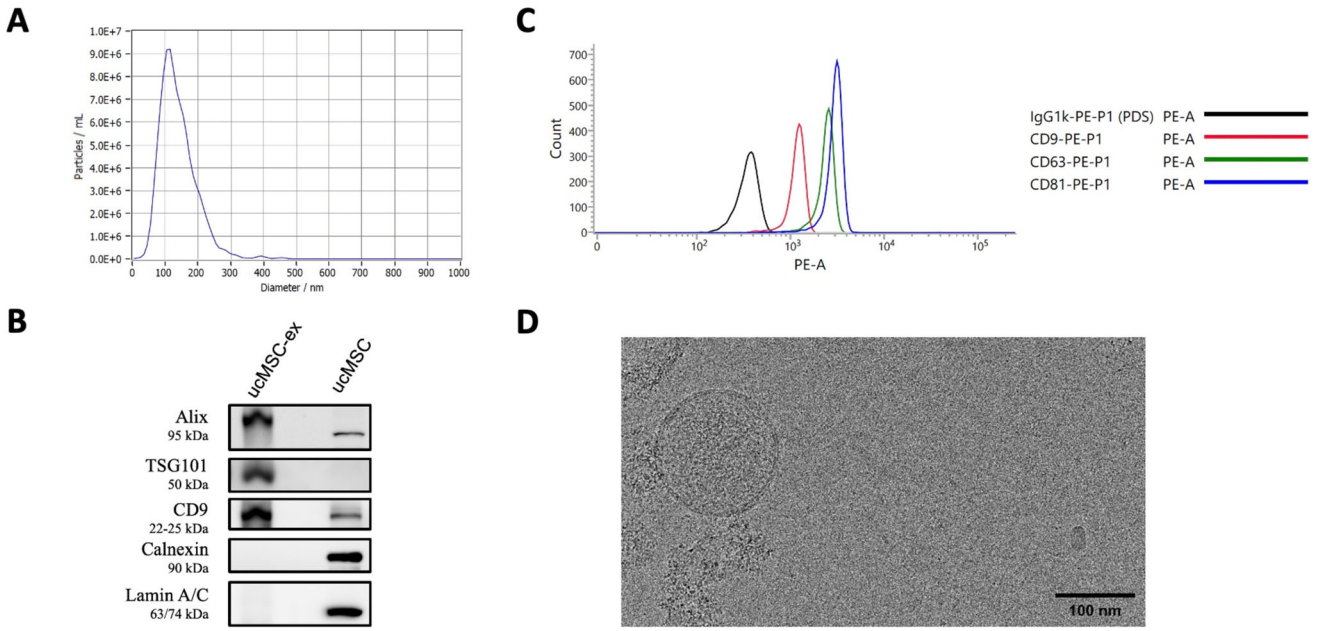


Fig. 2 Characterization of ucMSC-ex. **A** Particle size distribution profile of ucMSC-ex, measured through a nanoparticle tracking analysis on a ZetaView device. The median particle diameter was 112.3 nm at a peak concentration of 9.0E+6 particles/mL. **B** Western blotting of exosome markers (Alix, TSG101, and CD9, present in ucMSC-ex) and impurities (calnexin and lamin, present in cells only). **C** Flow cytometry of ucMSC-ex stained for CD9, CD63, and CD81. (**D**) Cryo-electron microscopy image of ucMSC-ex (scale bar: 100 nm)

exosome enrichment in the isolated fraction. By contrast, the cellular markers calnexin and lamin A/C were almost undetectable, indicating the high purity of the isolated exosome population. Flow cytometric analysis revealed that 87.27%, 85.38%, and 93.96% of the ucMSC-ex population expressed CD9, CD63, and CD81, respectively (Fig. 2C). Cryo-electron microscopy revealed a homogenous spherical vesicle, depicted next to a 100-nm scale bar in Figure 2D, consistent with the expected exosome morphology.

Distribution of ucMSC-ex in Vaginal Submucosa After Injection

Labeled ucMSC-ex were injected into the vaginal submucosa of the rats at the 3, 6, and 9 o'clock positions under general anesthesia by using a 24-gauge needle. Each injection was 0.2 mL in volume. After 24 h, the rats were euthanized under general anesthesia. Sufficient uptake of ucMSC-ex was observed under a Leica DMI6000 microscope (Leica, Heidelberg, Germany), revealing the clear internalization of fluorescence-labeled ucMSC-ex (Fig. 3).

Restoration of Histological Structure After ucMSC-ex Injection

The upper panel of Figure 4A presents the H&E evaluation of the vaginal tissue sections. In the N group, vaginal tissue exhibited a normal histological architecture with well-preserved epithelial layers and underlying lamina propria. The OVX group exhibited clear epithelial thinning and changes in the stromal structure, reflecting the effects of estrogen deficiency after ovariectomy. By contrast, the OVX+EXO group exhibited partial restoration of epithelial and stromal structure, suggesting that ucMSC-ex treatment had a regenerative effect. These findings highlight the potential therapeutic benefits of ucMSC-ex injections in the histological outcomes of vaginal tissue after ovariectomy.

Neocollagenesis After ucMSC-ex Injection

Figure 4 illustrates the histological analysis and quantification of vaginal tissue by using Masson's trichrome staining and Masson's score percentage. The lower panel of Figure 4A depicts representative images of stained vaginal tissue sections, where a blue stain indicates collagen deposition. Figure 4B displays a bar graph of expression levels observed through Masson's staining, quantifying the extent of collagen change. The OVX group exhibited a significant reduction in collagen deposition, indicating vaginal atrophy due to hypoestrogenism. By contrast, collagen deposition was significantly restored in the OVX+EXO group, suggesting a therapeutic effect. These results highlight the therapeutic effect of ucMSC-ex injections on stromal thickness and collagen deposition in vaginal tissue.

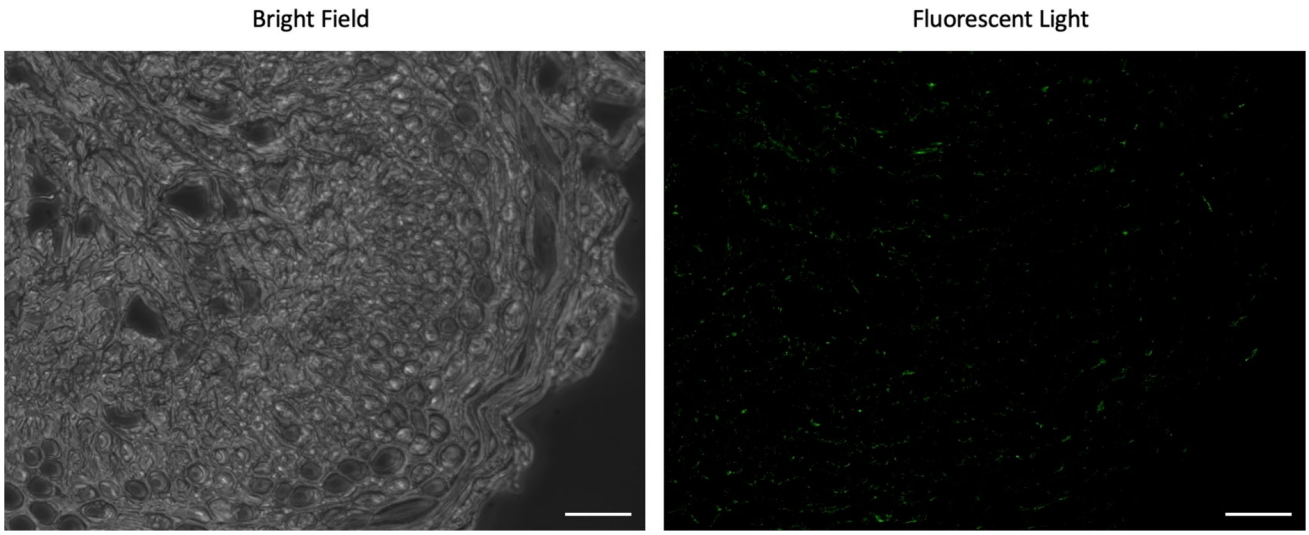


Fig. 3 Bright-field and fluorescence microscopy images of ucMSC-ex in the vaginal submucosa. Fluorescence confirmed successful labeling and sufficient uptake within the vaginal submucosa (scale bar: 100 nm)

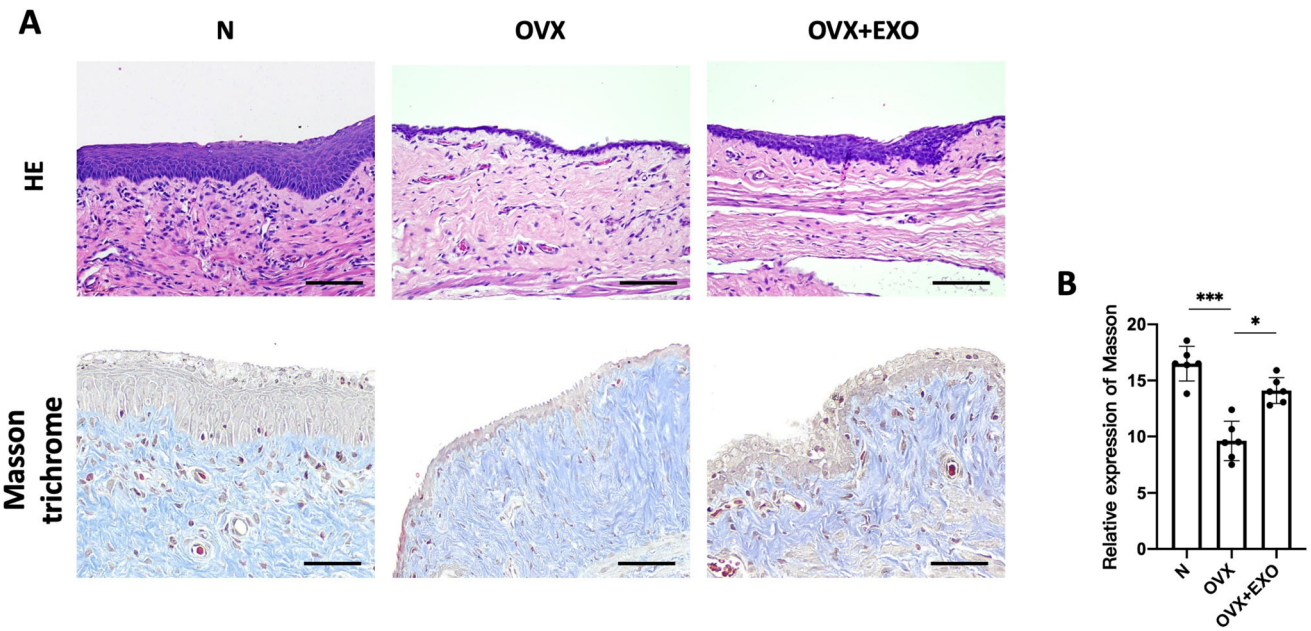


Fig. 4 H&E and Masson's trichrome analysis. **A** Representative images of vaginal sections stained with H&E and Masson's trichrome in each treatment group. Images were captured at a magnification of 200× (scale bar: 100 μm). **B** Quantitative analysis of collagen expression based on Masson's trichrome staining. The bar graph displays relative expression levels, with statistically significant differences indicated as * ($P < 0.05$) and *** ($P < 0.001$)

Neoangiogenesis After ucMSC-ex Injection

Figure 5 presents the IHC analysis and quantification results of angiogenesis in the vaginal tissue sections. Figure 5A depicts representative images of VEGF- and CD34-stained tissue, where dark and light brown staining indicate the presence of VEGF and CD34, respectively, in the epithelium and parts of the lamina propria. Figure 5B and Figure 5C display bar graphs quantifying VEGF and CD34 expression as average optical density values. For both angiogenesis markers, the N group exhibited baseline expression, whereas the OVX group exhibited a significant decrease in expression, suggesting impaired angiogenesis due to estrogen deficiency after ovariectomy. The OVX+EXO group exhibited significantly greater expression compared with the OVX group, suggesting that ucMSC-ex treatment facilitated neoangiogenesis and vascular repair. These findings indicate that ucMSC-ex can

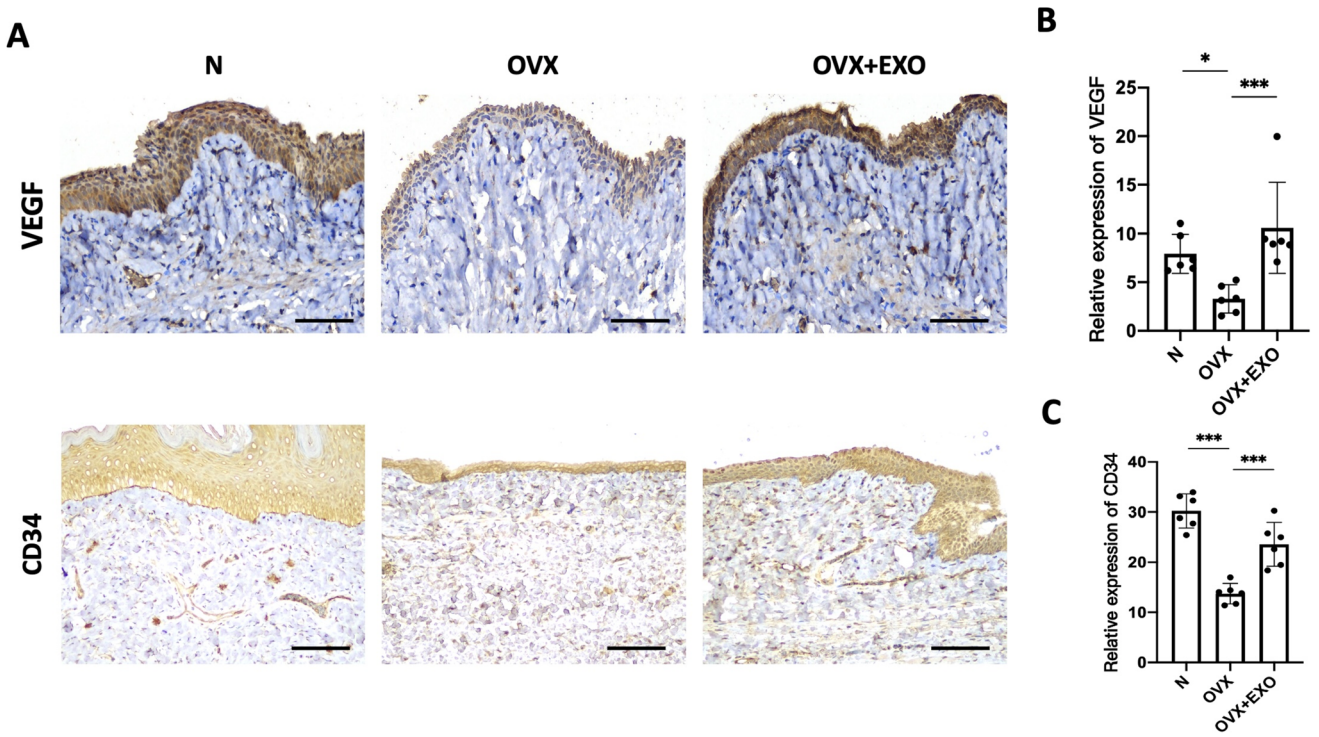


Fig. 5 VEGF and CD34 expression. **A** Representative images of IHC staining for VEGF and CD34 in vaginal tissue for each treatment group. Images were captured at a magnification of 200× (scale bar: 100 μm). Relative expression levels of **B** VEGF and **C** CD34 displayed as bar graphs, with significant differences marked as * ($P < 0.05$) and *** ($P < 0.001$)

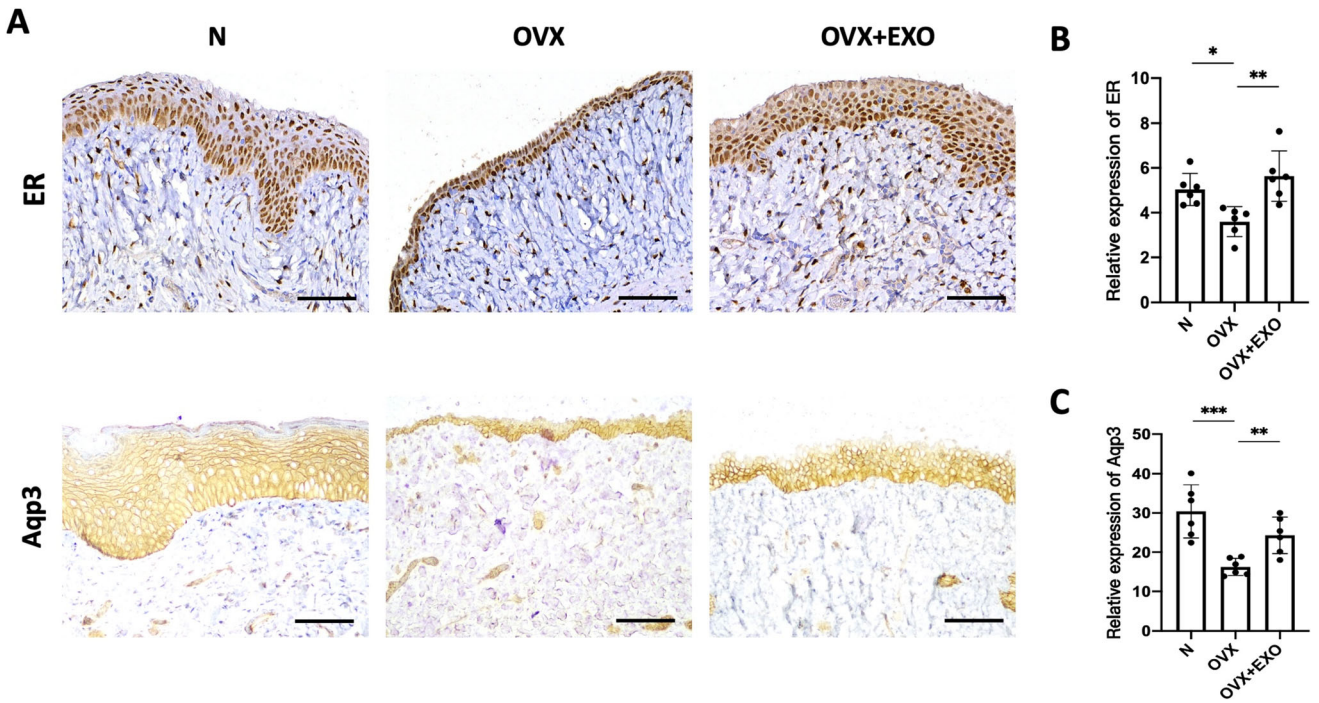


Fig. 6 ER and Aqp3 expression. **A** Representative images of IHC staining for ER and Aqp3 in vaginal tissue for each treatment group. Images were captured at a magnification of 200× (scale bar: 100 μm). Relative expression levels of **B** ER and **C** Aqp3 displayed as bar graphs, with significant differences marked as * ($P < 0.05$), ** ($P < 0.01$), and *** ($P < 0.001$)

effectively promote VEGF and CD34 expression, thereby potentially contributing to angiogenesis regulation.

Increased Estrogen Sensitivity and Vaginal Lubrication After ucMSC-ex Injection

Figure 6 presents the IHC analysis and quantification results of vaginal lubrication and estrogen sensitivity in the vaginal tissue sections. In Figure 6A, the dark and light brown stains in the epithelial layer represent the baseline expression of ER and Aqp3, respectively. Notably, the OVX group exhibited a significant reduction in ER and Aqp3 expression as a result of ovariectomy, as evidenced by a thin staining layer. After exosome injection, the OVX+EXO group displayed a major increase in staining intensity, suggesting that ucMSC-ex effectively restored ER and Aqp3 expression. The corresponding bar graphs in Figure 6B and Figure 6C quantify these observations, with the N group exhibiting baseline expression levels, the OVX group demonstrating the lowest levels, and the OVX+EXO group displaying substantial recovery of ER and Aqp3 expression. These findings demonstrate the efficacy of localized vaginal treatment with exosomes in modulating estrogen sensitivity in the vaginal epithelium and improving water transport for vaginal lubrication.

Improved Cellular Proliferation After ucMSC-ex Injection

Figure 7 displays the IHC analysis and quantification results of Ki67 expression, a marker of cellular proliferation, in the vaginal tissue sections. Figure 7A depicts representative images of Ki67-stained tissue, in which a brown stain indicates the presence of proliferating epithelial cells. Figure 7B presents bar graphs quantifying Ki67 expression as average optical density values in the epithelium. The results indicated that the N group exhibited baseline Ki67 expression, reflecting normal cellular proliferation. The OVX group exhibited reduced Ki67 expression, indicating decreased cellular proliferation due to the loss of ovarian function. After treatment, the OVX+EXO group exhibited significant restoration of Ki67 expression, indicating that ucMSC-ex enhanced cellular proliferation. These results suggest that ucMSC-ex injection effectively promotes cellular proliferation in vaginal tissues subjected to ovariectomy, highlighting the potential therapeutic benefits of ucMSC-ex in tissue repair and regeneration.

Repression of Oxidative Stress and Inflammation After ucMSC-ex Injection

Figure 8 displays the IHC analysis results of iNOS expression in the vaginal tissue sections. Figure 8A depicts representative images of iNOS-stained tissue, in which a brown stain indicates epithelial iNOS expression in the epithelium. Figure 8B presents bar graphs quantifying iNOS expression as average optical density values. The results indicated that the N group exhibited minimal iNOS expression, suggesting low baseline inflammation. By contrast, the OVX group exhibited high iNOS expression, indicating increased inflammation and oxidative stress due to estrogen deficiency after ovariectomy. Notably, the OVX+EXO group displayed a marked reduction in iNOS

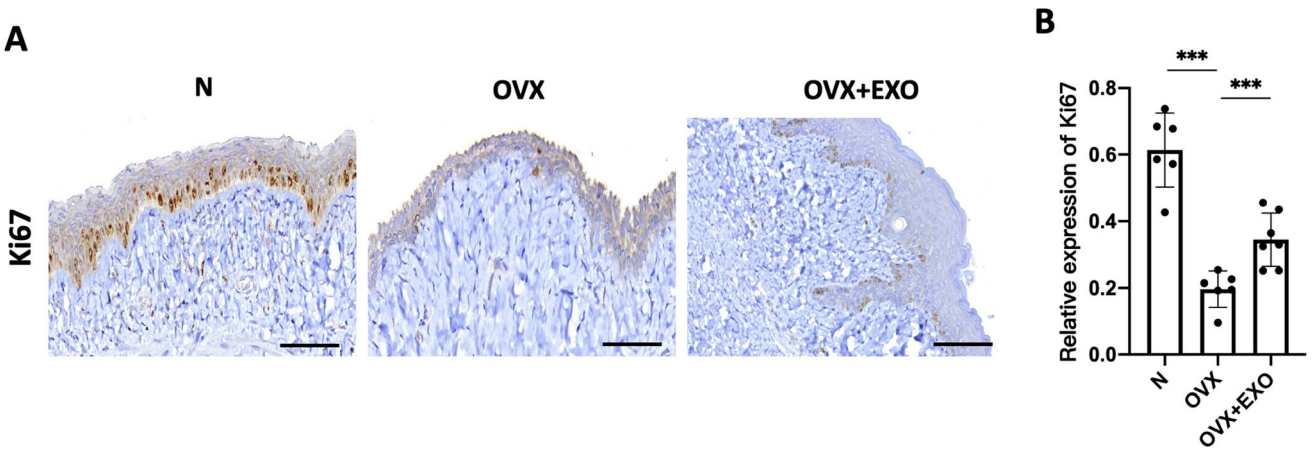


Fig. 7 Ki67 expression. **A** Representative images of IHC staining for Ki67 in vaginal tissue for each treatment group. Images were captured at a magnification of 200× (scale bar: 100 μm). **B** Bar graph illustrating the relative expression levels of Ki67, with significant differences marked as *** ($P < 0.001$)

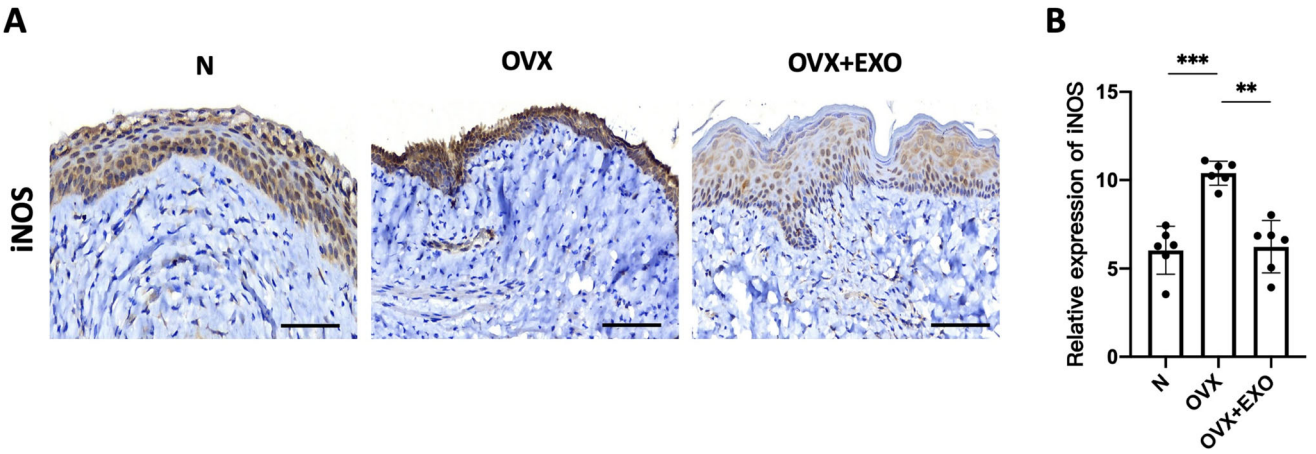


Fig. 8 iNOS expression. **A** Representative images of IHC staining for iNOS in vaginal tissue for each treatment group. Images were captured at a magnification of 200× (scale bar: 100 μm). **B** Bar graph illustrating the relative expression levels of iNOS, with significant differences marked as ** ($P < 0.01$) and *** ($P < 0.001$)

levels, suggesting the anti-inflammatory efficacy of ucMSC-ex treatment. Taken together, these findings suggest that ucMSC-ex treatment substantially mitigates inflammation in vaginal tissues subjected to ovariectomy.

Discussion

This study demonstrated the regenerative effects of a vaginal injection with ucMSC-ex in an ovariectomized rat model simulating menopause. Our findings provide histological evidence supporting the therapeutic potential of ucMSC-ex injection in alleviating the symptoms of GSM and postpartum sexual dysfunction, primarily through increased structural restoration, collagen formation, angiogenesis, estrogen sensitivity, vaginal lubrication, cellular proliferation, and anti-inflammation. Figure 9 presents a graphical summary of our study.

In recent years, local injections have become a widely accepted treatment for vulvovaginal atrophy during menopause [13]. However, clinical focus has typically been devoted to volumetric filling effects. Our previous work on regenerative effects highlighted the efficacy of adipose stem cell injections [14]. The effect of ucMSC-ex

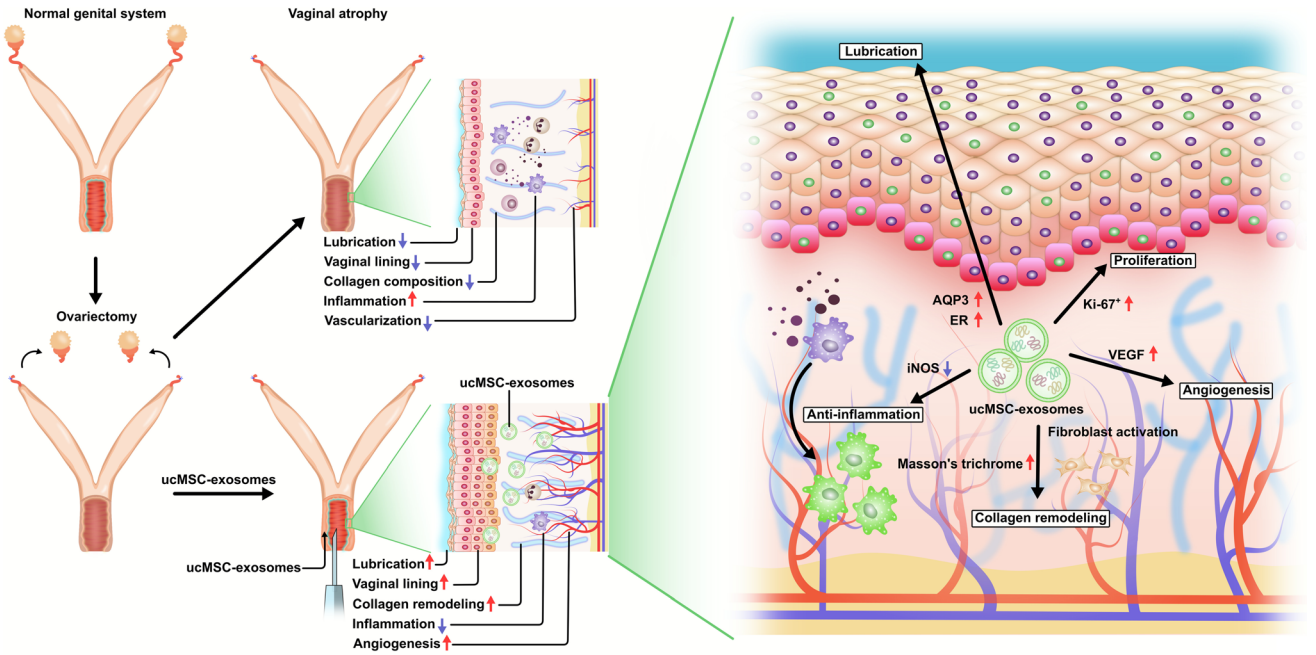


Fig. 9 Graphical summary of the regenerative effects of ucMSC-ex therapy on vaginal atrophy after ovariectomy

injection therapy on tissue regeneration has been widely studied in various medical conditions, including premature ovarian insufficiency, testicular aging, diabetic chronic wounds, and spinal cord injury [15–19]. In vaginal tissue, ucMSC-ex were observed to alter VK2 cell (vaginal epithelium) and fibroblast profiles to promote cell growth and function by modulating exosomal microRNAs [20–22]. Zhang et al. proposed the application of hydrogel injections loaded with ucMSC-ex into the vagina of ovariectomized rats, and they reported a positive histological change in vaginal atrophy with enhanced biomarkers of cell proliferation (Ki67) and angiogenesis (CD31) [22]. This intravaginal administration method involved the delivery of exosomes assisted by a hyaluronic acid hydrogel. In our study, we directly administered local ucMSC-ex injections into the vaginal submucosa of an ovariectomized rat model simulating a postmenopausal state. These injections enhanced epithelial cell proliferation (Ki67) and angiogenesis (VEGF and CD34) and improved estrogen sensitivity (ERs), vaginal lubrication (Aqp3), and anti-inflammatory effects (iNOS). H&E staining revealed that the ucMSC-ex injections significantly restored the structural integrity of the vaginal epithelium and underlying stroma, in stark contrast to the thinning and structural changes observed in the ovariectomized rats that did not receive ucMSC-ex treatment. Masson's trichrome staining revealed significant neocollagenesis in the stromal regions of vaginal tissues after ucMSC-ex injection, which was less pronounced in the untreated groups. These findings demonstrate that ucMSC-ex injections can promote extracellular matrix remodeling and structural recovery in the vagina in the presence of estrogen deficiency.

Vaginal dryness is among the most common symptoms of GSM resulting from low estrogen levels, making sexual intercourse a painful process. This dryness is primarily caused by vascularization in the vaginal mucosa, which affects local blood perfusion, thereby influencing local secretion [23, 24]. ERβ is distributed in the vascular smooth muscle cells of the vagina. Multiple studies have reported a decline in pelvic blood flow and Erβ levels in postmenopausal women with low vaginal lubrication [25–27]. Kim et al. and Zhu et al. argued that aquaporins (Aqps), a family of integral membrane proteins that function as channels facilitating water transport, can modulate vaginal lubrication by altering estrogen expression in the vaginal epithelium of rats undergoing ovariectomy or estrogen therapy [28, 29]. These studies suggest that the mechanism through which estrogen influences vaginal lubrication may involve modifying Aqps expression to regulate vaginal permeability, thereby modulating blood flow. However, the exact biochemical interactions underlying this mechanism remain to be further elucidated. In a previous study, we transplanted microautologous fat into the vulvovaginal area to treat vaginal dryness. This approach resulted in an increase in lubrication and dyspareunia domain scores of the Female Sexual Function Index and a significant increase in CD34 and ER expression in the treated vaginal tissue [14]. Many studies have confirmed the effects of ucMSC-ex on neoangiogenesis through different pathways [30–32]. Additionally, ucMSC-ex have been observed to increase estrogen levels and receptor sensitivity in perimenopausal ovarian tissue [33]. Zhang et al. used CD31 to quantify blood vessels in the vaginal tissue of ovariectomized rats, and they reported increased expression after hydrogel injection with ucMSC-ex [22]. In our study, IHC analysis revealed a major increase in VEGF, CD34, ER, and Aqp3 expression in the group treated with ucMSC-ex. Taken together, these results suggest that vaginal ucMSC-ex injections alleviate vaginal dryness by increasing angiogenesis and restoring estrogen responsiveness under conditions of estrogen deficiency.

Vaginal epithelial cell proliferation is marked by Ki67 and is regulated by estrogen through Wnt signaling pathways [34, 35]. Our IHC findings are consistent with those of Zhang et al., indicating a significant reduction in Ki67 expression in the vaginal tissue of ovariectomized rats, reflecting atrophic tissue remodeling caused by estrogen deficiency [22]. After ucMSC-ex injection, we observed an increase in Ki67 expression, indicating that ucMSC-ex can promote cellular proliferation to alleviate vaginal atrophy.

iNOS is a biomarker of oxidative stress that drives inflammation and apoptosis [36, 37]. Studies have indicated that local ischemia after birth injury or estrogen deficiency can activate iNOS expression, reducing trophicity in the lower urinary tract [38, 39]. Chen et al. demonstrated a positive association between the severity of stress urinary incontinence and iNOS expression in mouse urethra after vaginal dilatation and ovariectomy [40]. Despite these findings, the reasons underlying the altered iNOS expression in cases of vaginal atrophy, regardless of physical damage or metabolic imbalance, and the therapeutic effects of intravaginal estrogen cream remain unclear because of the lack of relevant studies [41]. In this study, iNOS overexpression was observed in the vaginal tissue of the OVX group. Treatment with ucMSC-ex significantly downregulated the expression of iNOS, indicating anti-inflammatory effects. These findings are consistent with those of Mao et al. and Yang et al., who reported that ucMSC-ex can mitigate inflammation and repair intestinal barriers [11, 42].

In our previous study, we discovered that ucMSC-ex injections had similar histological effects on vaginal tissue regeneration to those of the fat graft treatment applied in humans [14]. Both treatments improved histological structure and collagen deposition and markedly affected neoangiogenesis, cellular proliferation, and anti-inflammatory

response. These findings indicate that ucMSC-ex containing various bioactive molecules may display similar promise for vaginal regeneration to fat grafts.

In parallel with regenerative developments, technological innovations have increasingly transformed contemporary plastic surgery. Advanced tools such as 3-dimensional imaging, artificial intelligence-assisted analysis, and digital wound-assessment systems now contribute to more precise planning and outcome evaluation across both reconstructive and aesthetic domains [43–46]. Moreover, exosomes are emerging as key bioactive components in aesthetic and regenerative procedures, with recent clinical studies demonstrating their potential to enhance skin rejuvenation and tissue repair [47]. Future strategies may combine exosome therapy with existing regenerative modalities to maximize efficacy and safety. Finally, standardized patient-reported outcome measures (pROMs) such as FACE-Q and SCAR-Q have become indispensable for evaluating satisfaction and aesthetic results, aligning biological improvement with patient perception [48].

Despite the aforementioned promising results, our study has several limitations. First, because the study was conducted on animal models, the results may not be fully applicable to humans. Second, the exact cellular mechanisms underlying the effects of ucMSC-ex require further analysis, particularly regarding the interaction between exosomes and biomarkers in multiple pathways. Given that exosome-based therapies for vaginal atrophy and dryness remain in their early stages, future studies should explore these mechanisms in detail and evaluate the long-term safety and efficacy of ucMSC-ex in women with postmenopausal GSM or postpartum sexual dysfunction.

Conclusions

This animal study provides histological evidence for the regenerative effects of ucMSC-ex in the treatment of vaginal atrophy and dryness. Significant improvements were observed in histological structure, angiogenesis, estrogen sensitivity, vaginal lubrication, cellular proliferation, and inflammation, supporting the therapeutic potential of ucMSC-ex. These findings lay the foundation for future research and clinical applications aimed at improving the quality of life of women with GSM and postpartum sexual dysfunction.

Acknowledgements This study was supported by grants from Kaohsiung Municipal Ta-Tung Hospital, Kaohsiung, Taiwan (kmtth-113-012 and kmtth-109-041); the National Science and Technology Council (NSTC), Taipei City, Taiwan (NSTC 112-2314-B-037 -043 and 113-2314-B-037 -088 -MY3); Kaohsiung Municipal Siaogang Hospital, Kaohsiung, Taiwan (Proj-111-12, Proj-112-12, S-111-11, S-112-09, H-111-04, and H-112-04); Kaohsiung Medical University Hospital, Kaohsiung, Taiwan (KMUH113-3R30 and KMUH103-F302); Kaohsiung Medical University, Kaohsiung, Taiwan (ST-ST113016); Kaohsiung Medical University (ST-ST113016); and the Childhood Burn Foundation of the Republic of China, Taipei City, Taiwan. The authors would also like to express their gratitude to the Center for Laboratory Animals at Kaohsiung Medical University for providing excellent animal care.

Funding None of the authors had any commercial associations or financial relationships that may constitute a conflict of interest.

Declarations

Conflict of interest The authors declare that they have no conflicts of interest to disclose.

Human and Animal Rights This article does not contain any studies with human participants. Our animal protocols were approved by the Institutional Animal Care and Use Committee of Kaohsiung Medical University (IACUC 112047).

Informed Consent For this type of study, informed consent is not required.

References

1. Portman DJ, Gass ML, P. Vulvovaginal atrophy terminology consensus conference, Genitourinary syndrome of menopause: new terminology for vulvovaginal atrophy from the international society for the study of women's sexual health and the north american menopause society. Maturitas. 2014;79(3):349-54.
2. Signorello LB, et al. Postpartum sexual functioning and its relationship to perineal trauma: a retrospective cohort study of primiparous women. Am J Obstet Gynecol. 2001;184(5):881–8. discussion 888-90.
3. Pauls RN, Fellner AN, Davila GW. Vaginal laxity: a poorly understood quality of life problem; a survey of physician members of the International Urogynecological Association (IUGA). Int Urogynecol J. 2012;23(10):1435–48.
4. DiBonaventura M, et al. The association between vulvovaginal atrophy symptoms and quality of life among postmenopausal women in the United States and Western Europe. J Womens Health (Larchmt). 2015;24(9):713–22.
5. Coleman SR. Long-term survival of fat transplants: controlled demonstrations. Aesthet Plast Surg. 2020;44(4):1268–72.
6. Sulaica E, et al. Vaginal estrogen products in hormone receptor-positive breast cancer patients on aromatase inhibitor therapy. Breast Cancer Res Treat. 2016;157(2):203–10.
7. Luo G, et al. Promotion of cutaneous wound healing by local application of mesenchymal stem cells derived from human umbilical cord blood. Wound Repair Regen. 2010;18(5):506–13.
8. Lai RC, et al. Exosome secreted by MSC reduces myocardial ischemia/reperfusion injury. Stem Cell Res. 2010;4(3):214–22.
9. Walter MN, et al. Mesenchymal stem cell-conditioned medium accelerates skin wound healing: an in vitro study of fibroblast and keratinocyte scratch assays. Exp Cell Res. 2010;316(7):1271–81.
10. Basu J, Ludlow JW. Exosomes for repair, regeneration and rejuvenation. Expert Opin Biol Ther. 2016;16(4):489–506.
11. Yang S, et al. A novel therapeutic approach for inflammatory bowel disease by exosomes derived from human umbilical cord mesenchymal stem cells to repair intestinal barrier via TSG-6. Stem Cell Res Ther. 2021;12(1):315.
12. Ismail NH, et al. Modulation of vulvovaginal atrophy (VVA) by Gelam honey in bilateral oophorectomized rats. Front Endocrinol (Lausanne). 2023;14:1031066.

13. Moccia F, et al. Injection treatments for vulvovaginal atrophy of menopause: a systematic review. Aesthet Plast Surg. 2023;47(6):2788–99.
14. Lai YW, et al. Autologous fat grafting in female genital area improves sexual function by increasing collagenesis, angiogenesis, and estrogen receptors. Aesthet Surg J. 2023;43(8):872–84.
15. Pu X, et al. Human UC-MSC-derived exosomes facilitate ovarian renovation in rats with chemotherapy-induced premature ovarian insufficiency. Front Endocrinol (Lausanne). 2023;14:1205901.
16. Luo P, et al. Human umbilical cord mesenchymal stem cell-derived exosomes rescue testicular aging. Biomedicines. 2024. https://doi.org/10.3390/biomedicines12010098.
17. Yang J, et al. Umbilical cord-derived mesenchymal stem cell-derived exosomes combined pluronic F127 hydrogel promote chronic diabetic wound healing and complete skin regeneration. Int J Nanomedicine. 2020;15:5911–26.
18. Teng L, et al. Exosomes derived from human umbilical cord mesenchymal stem cells accelerate diabetic wound healing via promoting M2 macrophage polarization, angiogenesis, and collagen deposition. Int J Mol Sci. 2022. https://doi.org/10.3390/ijms231810421.
19. Luan Z, et al. Exosomes derived from umbilical cord-mesenchymal stem cells inhibit the NF-kappaB/MAPK signaling pathway and reduce the inflammatory response to promote recovery from spinal cord injury. J Orthop Surg Res. 2024;19(1):184.
20. Xu LM, et al. Exosomes from umbilical cord mesenchymal stromal cells promote the collagen production of fibroblasts from pelvic organ prolapse. World J Stem Cells. 2024;16(6):708–27.
21. Zhu Z, et al. Exosomes derived from human umbilical cord mesenchymal stem cells accelerate growth of VK2 vaginal epithelial cells through microRNAs in vitro. Hum Reprod. 2019;34(2):248–60.
22. Zhang T, et al. Delivering umbilical cord mesenchymal stem cell exosomes through hydrogel ameliorates vaginal atrophy in ovariectomized rats. Aging (Albany NY). 2023;15(23):14292–305.
23. Roberts H, Hickey M. Managing the menopause: an update. Maturitas. 2016;86:53–8.
24. Min K, et al. Selective P2Y2 receptor agonists stimulate vaginal moisture in ovariectomized rabbits. Fertil Steril. 2003;79(2):393–8.
25. Chen GD, et al. Estrogen receptor alpha and beta expression in the vaginal walls and uterosacral ligaments of premenopausal and postmenopausal women. Fertil Steril. 1999;71(6):1099–102.
26. Gebhart JB, et al. Expression of estrogen receptor isoforms alpha and beta messenger RNA in vaginal tissue of premenopausal and postmenopausal women. Am J Obstet Gynecol. 2001;185(6):1325-30. discussion 1330-1.
27. Traish AM, Botchevar E, Kim NN. Biochemical factors modulating female genital sexual arousal physiology. J Sex Med. 2010;7(9):2925–46.
28. Kim SO, et al. Effect of estrogen deprivation on the expression of aquaporins and nitric oxide synthases in rat vagina. J Sex Med. 2009;6(6):1579–86.
29. Zhu J, et al. Effects of estrogen deprivation on expression of aquaporins in rat vagina. Menopause. 2015;22(8):893–8.
30. Zhang Y, et al. Exosomes from human umbilical cord mesenchymal stem cells enhance fracture healing through HIF-1alpha-mediated promotion of angiogenesis in a rat model of stabilized fracture. Cell Prolif. 2019;52(2):e12570.
31. Zhang B, et al. Human umbilical cord mesenchymal stem cell exosomes enhance angiogenesis through the Wnt4/beta-catenin pathway. Stem Cells Transl Med. 2015;4(5):513–22.
32. Liu J, et al. Exosomes derived from human umbilical cord mesenchymal stem cells accelerate cutaneous wound healing by enhancing angiogenesis through delivering angiopoietin-2. Stem Cell Rev Rep. 2021;17(2):305–17.
33. Alkhrait S, et al. Exosome therapy: a novel approach for enhancing estrogen levels in perimenopause. Int J Mol Sci. 2024. https://doi.org/10.3390/ijms25137075.
34. Benitez-Roig V, et al. Clinical and laboratory results in vaginal wall restoration using a fractional-pixel-CO(2) laser: histological findings and changes in the Ki67 protein and telomere length. Lasers Med Sci. 2023;38(1):206.
35. Ali A, et al. Cell lineage tracing identifies hormone-regulated and Wnt-responsive vaginal epithelial stem cells. Cell Rep. 2020;30(5):1463-1477 e7.
36. Nakazawa H, et al. iNOS as a driver of inflammation and apoptosis in mouse skeletal muscle after burn injury: possible involvement of Sirt1 S-nitrosylation-mediated acetylation of p65 NF-kappaB and p53. PLoS ONE. 2017;12(1):e0170391.
37. Karpuzoglu E, et al. Estrogen up-regulates inducible nitric oxide synthase, nitric oxide, and cyclooxygenase-2 in splenocytes activated with T cell stimulants: role of interferon-gamma. Endocrinology. 2006;147(2):662–71.
38. Game X, et al. Estradiol increases urethral tone through the local inhibition of neuronal nitric oxide synthase expression. Am J Physiol Regul Integr Comp Physiol. 2008;294(3):R851–7.
39. Andersson KE, Persson K. Nitric oxide synthase and nitric oxide-mediated effects in lower urinary tract smooth muscles. World J Urol. 1994;12(5):274–80.
40. Chen HY, et al. Synergistic effect of vaginal trauma and ovariectomy in a murine model of stress urinary incontinence: upregulation of urethral nitric oxide synthases and estrogen receptors. Mediators Inflamm. 2014;2014:314846.
41. Illston JD, et al. Low-dose 17-beta-estradiol cream for vaginal atrophy in a cohort without prolapse: serum levels and vaginal response including tissue biomarkers associated with tissue remodeling. Maturitas. 2015;81(4):475–9.
42. Mao F, et al. Exosomes derived from human umbilical cord mesenchymal stem cells relieve inflammatory bowel disease in mice. BioMed Res Int. 2017;2017:5356760.
43. Guarro G, et al. Wounds morphologic assessment: application and reproducibility of a virtual measuring system, pilot study. Acta Biomed. 2021;92(5):e2021227.
44. Winter E, et al. The LACE+ index as a predictor of 30-day patient outcomes in a plastic surgery population: a coarsened exact match study. Plast Reconstr Surg. 2020;146(3):296e–305e.
45. Guarro G, et al. The modified TIME-H scoring system, a versatile tool in wound management practice: a preliminary report. Acta Biomed. 2021;92(4):e2021226.
46. Guarro G, Fabrizio T. Indications for and limitations of reconstruction of auricular defects with the "mid-moon flap" and evaluation of outcome by the Aesthetic Numeric Analogue Score. Plast Reconstr Surg Glob Open. 2023;11(7):e5152.
47. Svolacchia F, et al. Exosomes and signaling nanovesicles from the nanofiltration of preconditioned adipose tissue with skin-B((R)) in tissue regeneration and antiaging: a clinical study and case report. Medicina (Kaunas). 2024. https://doi.org/10.3390/medicina60040670.
48. Ottenhof MJ, et al. The use of the FACE-Q aesthetic: a narrative review. Aesthet Plast Surg. 2022;46(6):2769–80.

Publisher's Note Springer Nature remains neutral with regard to jurisdictional claims in published maps and institutional affiliations.

Springer Nature or its licensor (e.g. a society or other partner) holds exclusive rights to this article under a publishing agreement with the author(s) or other rightsholder(s); author self-archiving of the accepted manuscript version of this article is solely governed by the terms of such publishing agreement and applicable law.